ACS Catalysis

Research Article

pubs.acs.org/acscatalysis

Kinetics and Thermochemistry of C_4–C_6 Olefin Cracking on H-ZSM-5

Cha-Jung Chen, Srinivas Rangarajan, Ian M. Hill, and Aditya Bhan*

Department of Chemical Engineering and Materials Science, University of Minnesota-Twin Cities, 421 Washington Avenue SE, Minneapolis, Minnesota 55455, United States

Supporting Information

ABSTRACT: C_4–C_6 olefin β-scission rate constants were inferred from experimental studies at 773–813 K and <15% conversion by considering every C_4–C_6 olefin isomer and all available β-scission modes: 2° to 2° (C), 1° to 3° and 3° to 1° (E), 1° to 2° and 2° to 1° (D), and 1° to 1° (F). Group contribution methods were implemented to assess adsorption enthalpies and entropies of C_4–C_6 olefin isomers on H-ZSM-5 via the development of group correction terms for surface alkoxides; a linear dependence of enthalpy (or entropy) of formation difference between a surface alkoxide and a gas-phase alkane on carbon number was considered. Tertiary alkoxides have the smallest adsorption constants among surface adsorbates, and the resulting low coverage of highly substituted alkoxides restricts their contribution to alkene cracking pathways. Intrinsic β-scission rate constants (k_E:k_C:k_D:k_F ratio of 1094:21:8:1 at 783 K) and activation energies (E_{inE} < E_{inC} < E_{inD} < E_{inF}) from experimentally observed effluent compositions of C_4–C_6 olefin cracking consistent with computational studies were derived after rigorously accounting for adsorption constants and surface coverages of each C_4–C_6 olefin isomer. These results demonstrate that shape selectivity constraints prevent equilibration of surface alkoxides on surfaces under reaction conditions relevant for alkene cracking and present a quantitative description of C–C bond cracking reactions of olefins catalyzed by solid acids.

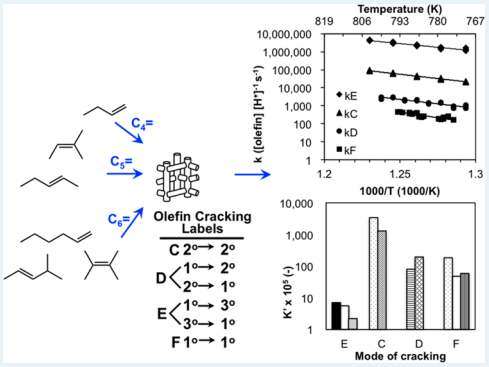

KEYWORDS: *olefin cracking, ZSM-5, β-scission, group additivity, group correction, alkoxides*

1. INTRODUCTION

Olefin cracking is ubiquitous in acid-catalyzed reactions of olefins, which is important especially in processes that upgrade light olefinic gases to high-quality gasoline products such as Lurgi's Methanol to Propylene process[1] and the MOGD[2] (Mobil olefins-to-gasoline and distillate) process. Quann et al.[3] in studying light olefin (C_3–C_6) conversion on H-ZSM-5 over a temperature range of 477–655 K and a pressure range of 0.01–100 bar observed products ranging from C_5 to C_{30}, showing the complexity of acid-catalyzed reactions of olefins, which has been described by Pines[4] using the term "conjunct polymerization". Bessell and Seddon[5] noted that light olefin conversion on H-ZSM-5 occurred via successive isomerization, oligomerization, cracking of higher-order oligomers, and hydrogen transfer. Guisnet et al.[6] also found that 1-butene conversion on medium pore zeolites like H-FER, H-TON, H-EU-1, and H-MFI at 623 K is highly selective to isobutene, propene, and pentenes as a result of a sequence of oligomerization, isomerization, and cracking steps. These parallel reactions (Scheme 1a) have hence precluded detailed experimental kinetic studies of olefin cracking on acidic zeolites.

β-Scission is the predominant mechanism for olefin cracking on solid acid catalysts.[7−10] It involves the protonation of an olefin to form an alkoxide intermediate with the framework oxygen atom; subsequently, the β C bond relative to the adsorbed carbon breaks to form a smaller olefin and a carbocationic hydrocarbon, which forms another olefin via one of three pathways (Scheme 2):[11] (1) immediate transfer of hydrogen back to the zeolite, (2) physisorption on the zeolite with subsequent hydrogen transfer, or (3) chemisorption followed by β-hydrogen elimination. A recent computational study that accounts for dispersive corrections on an MFI supercell containing the full crystal structure shows that the transition state for β-scission occurs when the α C and β C are fully sp^2 hybridized.[11]

Weitkamp et al.[12] developed a nomenclature to describe the various modes of olefin cracking based on carbenium ion types involved in products and reactants when studying C_9–C_{16} *n*-alkane hydrocracking on Pt/H-ZSM-5. Buchanan et al.[13] extended this nomenclature (Scheme 1b) in studying the relative rates of monomolecular alkene cracking for C_5–C_8 olefins on H-ZSM-5 at 783 K. Olefin isomerization was postulated to precede alkene cracking so an equilibrium distribution of alkene isomers was considered starting from an *n*-alkene feed. The ratio of rates for C_5:C_6:C_7:C_8 alkene cracking was evaluated to be 1:24:192:603, which was rationalized on the basis of carbenium ion stability wherein a more energetically favorable mode of cracking becomes available for larger olefins. Although larger hydrocarbons can access more stable transition states, we show here that adsorption constants of alkoxide intermediates that lead to these more stable transition states, however, are low, and the

Received: January 25, 2014
Revised: May 27, 2014
Published: June 17, 2014

   dx.doi.org/10.1021/cs500119n | ACS Catal. 2014, 4, 2319–2327

Scheme 1. (a) Olefin Reactions on a Zeolite Acid Site, (b) Modes of β-Scission and Their Associated Labels, and (c) β-Scission Modes for Pentene Cracking[a]

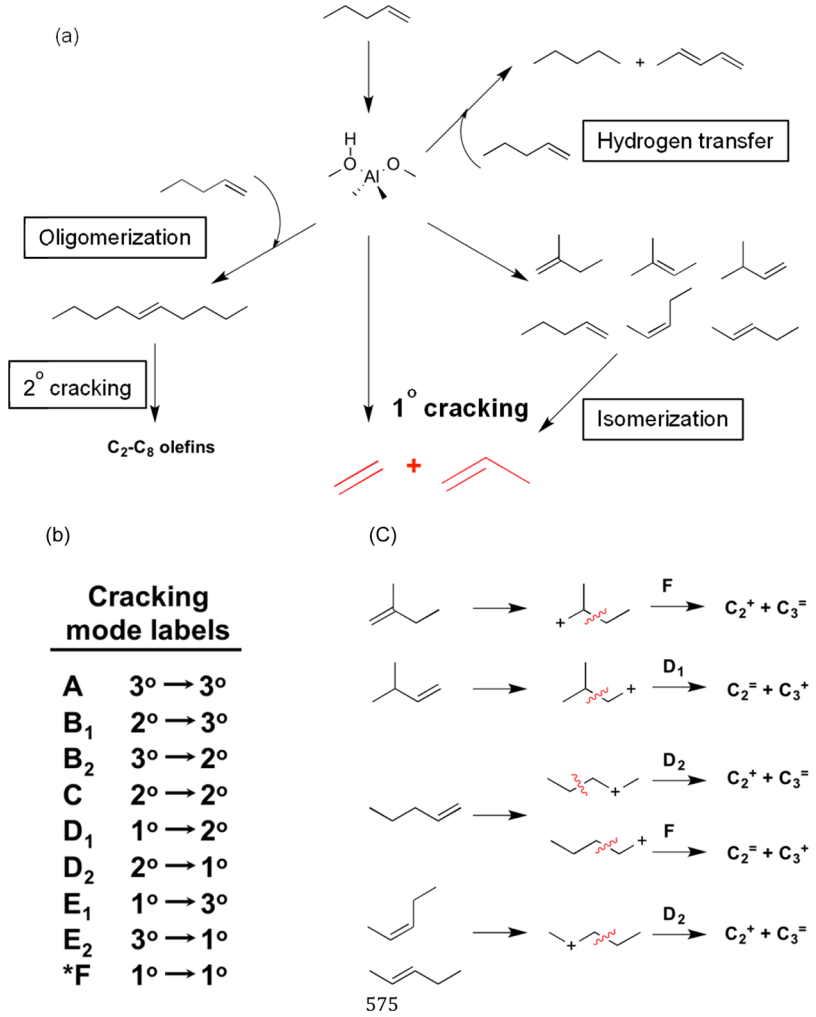

[a]The asterisk denotes an undocumented label.

Scheme 2. Three Pathways of Forming Olefin Cracking Products from the Transition State of β-Scission: (1) Direct Hydrogen Transfer, (2) Physisorption of β C, Followed by Hydrogen Transfer, and (3) Chemisorption of the β C, Followed by β-Hydrogen Elimination [reproduced from ref 11 (copyright 2013 American Chemical Society)]

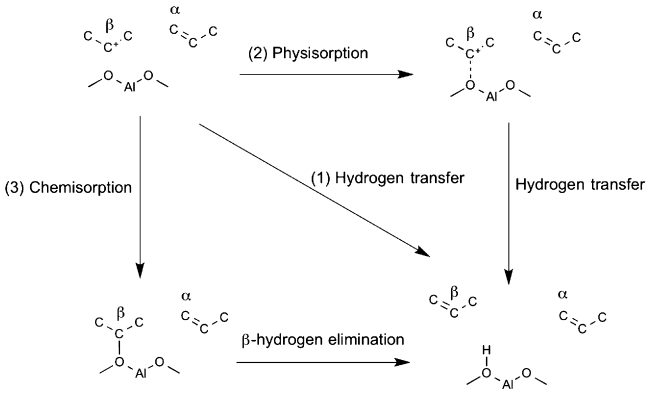

contribution of such modes may not be the predominant olefin cracking pathway (section 3.4).

Intrinsic activation barriers for different β-scission modes were found to depend on the substitution order of the carbenium ions involved in the reactant and transition states.[11,13−16] Frash et al.[14] investigated β-scission mechanisms on zeolites using density functional theory (DFT) and *ab initio* Hartree−Fock calculations on 1T and 3T clusters and showed that the β-scission activation barrier of 2-pentoxide was 20.9 kJ mol^{-1} lower than that for 1-butoxide, indicating that the additional methyl group stabilizes the carbocationic transition state with respect to the reactant state. Mazar et al.[11] investigated β-scission modes A−E (Scheme 1b) for various C_6 and C_8 olefin isomers over H-ZSM-5 using dispersion-corrected density functional theory (PBE-D). The barrier heights for β-scission were found to monotonically increase with an increase of the change in the charge of the β C going from the physi- or chemisorbed reactant state to the transition state. Mazar et al.[11] also noted that the substitution order of the transition state has a stronger influence on the intrinsic activation energy than the reactant state.

Gas-phase olefins were observed to undergo multiple protonation and deprotonation and hydride shifts (almost barrierless) or methyl shifts (intrinsic activation energy of ∼10 kJ mol^{-1}) before cracking into smaller olefins.[10,13,17] It has been

dx.doi.org/10.1021/cs500119n | ACS Catal. 2014, 4, 2319−2327

shown both experimentally and computationally that hydride shifts of olefins on acid catalysts occur easier than methyl group migration, which is easier than direct branching rearrangements.[10,18−20] Buchanan et al.[10] studied 1-hexene (0.5 atm partial pressure) conversion on H-ZSM-5 and found that, at 589 K, 4% of the feed cracked to lighter olefins while 91% of the 1-hexene converted into other C_6 isomers, with concentrations of linear hexenes being higher and those of more branched isomers being lower than those predicted from gas-phase equilibrium calculations. Quann et al.[3] have also reported that the observed hexene isomer distribution when feeding 1-hexene at 500 K and low conversion (3%) on H-ZSM-5 deviated significantly from the predicted equilibrium distribution. The fast isomerization of olefins on acidic zeolites before cracking, therefore, does not guarantee a gas-phase equilibrium distribution among the isomers,[10,13,17,21] because size restrictions within microporous voids restrain the formation of certain branched molecules that are thermodynamically preferred.[3,10,21,22] Our findings in this work confirm the observation that equilibration of olefin isomers does not occur for C_4−C_6 olefin conversion on H-ZSM-5 at 783−813 K. We quantify the extent of alkene isomerization and account for the adsorption constants and cracking modes of each olefin isomer in studying olefin cracking to elucidate β-scission kinetics under differential reaction conditions (section 2.4).

Group additivity methods, originally proposed by Benson,[23] have been used for rapid estimation of thermodynamic data of gaseous molecules from a limited set of parameters, called group additivity values (GAVs), in which a group is defined as a central atom with ligands. Group correction methods were developed to encompass structural features of the molecules that are difficult to incorporate into a group additivity scheme, such as nonbonded interactions, non-next-nearest-neighbor interactions, ring strain effects, and symmetry corrections.[23] This semiempirical method has been implemented extensively for gas-phase organic compounds and radicals;[24−26] the application in the estimation of thermochemical properties of surface species was first developed by Kua et al.[27] for examining adsorption of hydrocarbons on metal surfaces and was further extended by Salciccioli et al.[28,29] for studying the conversion of oxygenates (carboxylic acids, ethers, esters, etc.) on group VIII transition metals. Linear scaling relationships for relating the binding energy of a species on one transition metal surface to that of another were developed by Nørskov and co-workers[30,31] to semiempirically estimate reaction energies. Thermochemical data for surface species on zeolites, however, are scarce and derived mostly from DFT calculations,[32−36] which precludes detailed kinetic studies of hydrocarbon reaction systems on zeolites comprising large numbers of reactions. Our study proposes linear group correction relationships based on thermochemical properties of gas-phase alkanes to calculate the enthalpy and entropy of formation of surface alkoxide species on H-ZSM-5. Thereby, olefin adsorption enthalpy and entropy values can be obtained to rigorously assess the contributions of adsorption and kinetics to observed β-scission rates for C_4−C_6 olefin cracking.

In this work, intrinsic rate constants and activation energies of β-scission modes C−F were analytically inferred from butene, pentene, and hexene cracking at 773−813 K on H-ZSM-5, accounting for the concentration of each alkene isomer in the effluent stream. Linear relationships for estimating the enthalpy and entropy of formation for surface alkoxides were proposed to assess adsorption constants for each olefin isomer based on group additivity methods implemented in Rule Input Network Generator (RING).[37,38] Dominant olefin cracking pathways and kinetic parameters for the different modes of β-scission were assessed and are compared with recent computational chemistry reports to infer that (i) intrinsic β-scission rate constants and activation energies follow the rules of carbenium chemistry ($E_{inE} < E_{inC} < E_{inD} < E_{inF}$ and k_E:k_C:k_D:k_F ratio of 1094:21:8:1 at 783 K), and (ii) tertiary alkoxides have the lowest adsorption constants among other surface adsorbates, restricting thereby the contribution from mode E cracking.

2. MATERIALS AND METHODS

2.1. Thermochemistry for Surface Alkoxides on H-ZSM-5. The enthalpy and entropy of formation for alkoxides on H-ZSM-5 were calculated using RING, developed by Rangarajan et al.,[37−39] which incorporates a representation of surface intermediates and accommodates elementary step reaction rules to describe chemical transformations of organic molecules on surfaces. The inputs to RING are (i) the initial reactants and (ii) a set of reaction rules describing the chemistry. Additional inputs, including group additivity rules and group correction rules, are used to calculate thermochemical quantities of molecules and reactions on the fly. RING outputs an exhaustive list of species and reactions generated from the reactants and reaction rules provided. The GAVs for gas-phase molecules in RING were taken from refs 23 and 40−42. In this study, group correction terms for surface species on H-ZSM-5 were developed on the basis of the structural similarity between gas-phase alkanes and surface alkoxide intermediates, wherein an alkoxide replaces a hydrogen atom in the corresponding alkane with the framework oxygen (Scheme 3). Linear relationships between carbon number and enthalpy and entropy differences between alkoxides and alkanes were assessed as follows (Scheme 3).

Scheme 3. Representation of Enthalpies Involved in Developing Linear Relationships for Alkoxides, Which Is Based on the Structural Similarity between Gas-Phase Alkanes (underlined) and Surface Alkoxide Intermediates (underlined) (i.e., an alkoxide replaces a hydrogen atom in the corresponding alkane with the framework oxygen)

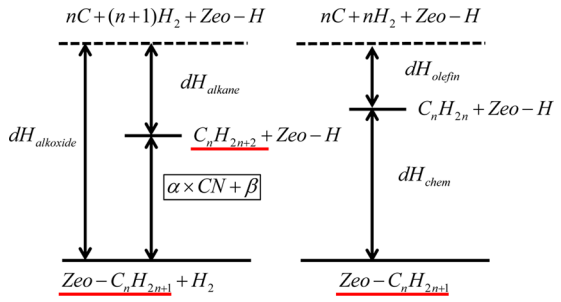

The enthalpy of formation for a surface alkoxide species was calculated as

$$dH_{alkoxide} = dE_{chem} + 12 + dH_{olefin} \quad (1)$$

where $dH_{alkoxide}$ and dH_{olefin} are the enthalpy of formation of the alkoxide and the olefin, respectively, dE_{chem} is the electronic energy of olefin chemisorption on H-ZSM-5, and 12 (kJ mol^{-1}) is the correction term relating the chemisorption electronic energy to the chemisorption enthalpy resulting from the contribution of zero point vibrational energy and thermal

dx.doi.org/10.1021/cs500119n | ACS Catal. 2014, 4, 2319−2327

corrections.[33] Values of dH_{olefin} (kJ mol^{-1}) were taken from RING at 298 K and dE_{chem} from ref 33 for secondary and internal secondary alkoxides at 298 K. For tertiary alkoxides, $dH_{alkoxide}$ values were directly calculated from $dH_{alkoxide} = -21.7 \times CN - 40.9$ as reported by Nguyen et al.[32]

The enthalpy difference between an alkoxide and an alkane was found to be linearly dependent on carbon number for secondary, internal secondary, and tertiary alkoxides (eq 2); parameters used for finding the relationships are reported in the Supporting Information. A linear relationship for primary alkoxides was determined using the same slope that was used for secondary alkoxides with the intercept determined by referencing values for ethane computed using RING to that computed for ethoxide formation by Nguyen et al.[33] using density functional theory.

$$dH_{alkoxide} - dH_{alkane} = \alpha \times CN + \beta \quad (2)$$

where $dH_{alkoxide}$ is as defined in eq 1 and dH_{alkane} at 298 K was calculated using RING.

A linear relationship for the entropy of formation of alkoxides was found in a similar manner and is reported in eq 3:

$$dS_{alkoxide} - dS_{alkane} = \gamma \times CN + \eta \quad (3)$$

where $dS_{alkoxide}$ values (J K^{-1} mol^{-1}) were taken from ref 33 at 298 K for secondary and internal secondary alkoxides and dS_{alkane} values at 298 K were calculated using RING.

The assumptions in this analysis are (i) linear relationships found for linear olefins are applicable for branched olefins and (ii) the thermochemical values reported at 298 K are valid at higher temperatures.

2.2. Catalyst Preparation. A ZSM-5 sample from Zeolyst International (CBV 8014) was sieved in the ammonium form to obtain aggregate particle sizes between 180 and 425 μm (40−80 mesh). The Si:Al ratio for the ZSM-5 sample was determined by elemental analysis using inductively coupled plasma optical emission spectrometry (ICP-OES) to be 42.6 (performed by Galbraith Laboratories in Knoxville, TN). Results from elemental analysis, N_2 adsorption experiments, and X-ray diffraction are reported in Table S1 and Figure S1 of the Supporting Information. The samples were treated in flowing dry air (1.67 cm^3 s^{-1}, ultrapure, Minneapolis Oxygen; temperature ramp of 0.0167 K s^{-1}) at 773 K for 4 h to thermally decompose NH_4^+ to H^+ and NH_3(g) and form protonated zeolites, denoted as H-ZSM-5. Chiang et al.[43] performed dimethyl ether (DME) titration experiments at 438 K over the ZSM-5 sample used in this study and showed that 0.5 ± 0.05 DME molecule is adsorbed per acid site, indicating that the Brønsted acid site concentration is nearly identical to the Al content determined via ICP-OES.

2.3. Steady-State Catalytic Reactions of Olefin Cracking. Steady-state olefin cracking reactions were conducted in a 10 mm inner diameter packed-bed quartz reactor at 180 kPa (Table 1). The catalyst was supported on a quartz frit at the bottom of the reactor, and the temperature was controlled using a furnace (National Electric Furnace FA120 type) connected to a Watlow Temperature Controller (96 series). The reactor temperature was measured using a K type thermocouple placed in a thermal well in the middle of the reactor bed. Samples (the milligram catalyst sample was obtained from a previously diluted catalyst mixture, which was further diluted in quartz sand to 0.8 g total weight in the reactor) were pretreated in flowing He (2.17 cm^3 s^{-1}, ultrapure, Minneapolis Oxygen) at 773 K (temperature ramp of 0.033 K s^{-1}) for 6 h. A mixture of methane and argon (1:99, Matheson) was used as an internal standard and was combined with the olefinic reactant: 1-butene (Matheson Tri-Gas, chemical purity grade), 2-pentene or 2-methyl-2-butene (Sigma-Aldrich, analytical grade), or 1-hexene, *trans*-4-methyl-2-pentene, or 2,3-dimethyl-2-butene (Sigma-Aldrich, analytical grade). Pentene and hexene isomers were introduced using a syringe pump (kdScientific) with He as the carrier gas to maintain the desired total flow rate (2.3−3.3 cm^3 s^{-1}). The reactor effluent composition was monitored using a gas chromatograph−mass spectrometer (GC−MS, Agilent 7890-5975C) through a methyl-siloxane capillary column (HP-1, 50.0 m × 320 μm × 0.52 μm) connected to a flame ionization detector and a (5% phenyl)-methylpolysiloxane capillary column (HP-5, 30.0 m × 320 μm × 0.52 μm) connected to a mass spectrometer.

Table 1. Reaction Conditions for Olefin Cracking over H-ZSM-5

olefin	conversion (%)	temperature range (K)	amount of catalyst (mg)	olefin pressure (Pa)	modes of cracking
1-butene	<0.1	783−803	0.6	17	F
2-pentene	<1	773−803	0.3	13	D, F
2-methyl-2-butene	<1	773−803	0.3	13	D, F
1-hexene	<10	773−803	0.3	38	C−F
trans-4-methyl-2-butene	<15	773−813	0.3	34	C−F
2,3-dimethyl-2-butene	<3	773−813	0.3	48	C−F

2.4. Method for Obtaining Intrinsic β-Scission Rate Constants. Cracking of butene, pentene, and hexene involve β-scission modes C−F (Table 1) and forms four sets of cracking products, which can be formulated into four independent equations (eqs 7−10) having four β-scission rate constants that are assumed to be independent of the olefin carbon chain length based on the consideration that in each β-scission mode a similar C−C bond is fragmented in a molecule with a similar carbon backbone structure (section 3 of the Supporting Information). Submodes with the same carbenium ions involved, for instance, 1° to 3° (E_1) and 3° to 1° (E_2), are lumped as a single mode to reduce the number of unknowns for the four equations. Simultaneously solving four equations from the four sets of cracking products allows an analytical solution for calculating the rate constants of β-scission modes C−F without parameter estimation. The equations involved are shown below with 2-pentene feed as an example.

The propene synthesis rate from 2-pentene cracking can be expressed as

$$r_{C_3^=} = \sum_j k_i K_j (1 - \theta) P_j \quad (4)$$

where $r_{C3}^=$ is in s^{-1}; P_j is the partial pressure of pentene isomer j, resulting from 2-pentene isomerization (in Pa) measured in the effluent stream; k_i is the rate constant of mode i (mode D or F) that corresponds to pentene isomer j (in s^{-1}); K_j is the adsorption equilibrium constant of isomer j (in Pa^{-1}) evaluated at reaction temperature extrapolating adsorption enthalpies and entropies obtained at 298 K; and θ is the fractional surface coverage of all pentene isomers, with the consideration that olefin chemisorption is quasi-equilibrated.[13]

dx.doi.org/10.1021/cs500119n | ACS Catal. 2014, 4, 2319−2327

The mass balance of a catalyst bed in a continuous-flow reactor under differential conversion conditions (<15% conversion) is

$$F_{C_3^=\text{out}} - F_{C_3^=\text{in}} = (r_{C_3^=})w_T \quad (5)$$

where w_T is the total number of acid sites.

$F_{C3^=_{in}}$ is zero; $F_{C3^=_{out}}$ can be measured in the effluent stream, and $r_{C3^=}$ is expressed as eq 4. Subsequently, eq 5 becomes

$$F_{C_3^=\text{out}} = [\sum_j k_i K_j (1-\theta) P_j] w_T \quad (6)$$

The enthalpy and entropy of each olefin isomer were calculated using RING by group additivity with group correction methods as described above (section 2.1) to calculate the equilibrium constant, K_j. The fractional surface coverage θ was determined by considering the highest concentrations of the adsorbed species in the system: olefin feed pressure at the inlet and partial pressure of the cracking products at the outlet. θ was $<10^{-6}$ for butene, pentene, and hexene cracking, demonstrating that the catalyst surface is predominantly uncovered under the reaction conditions employed in this research.

2.5. Assessment of Reactor Bed Dilution. Dilution of the catalyst bed would cause deviation of the conversion from an undiluted bed, which is a result of local bypass effects when catalyst particles are discretized in a local area by the surrounding inert. Berger et al.[44] investigated the relation between the extent of bed dilution and the deviation of the observed chemical conversion using a random particle distribution model and a first-order irreversible reaction: N_2O decomposition on a Co−La−Al mixed oxide. They found that the deviation would increase with the diluent fraction but decrease with conversion. Berger et al.[44] showed that bypass effects can be neglected when the dimensionless residence time (<0.25) and fractional conversion (<15%) in the bed are low. The deviation of fractional conversion was taken to be negligible in this study because of the observed conversions (<15%) and residence times (<0.03) remaining within the limits of differential conversion as outlined by Berger et al.[44]

3. RESULTS AND DISCUSSION

Linear relationships used for calculating the enthalpy and entropy of surface alkoxides are shown in Table 2, and they are archived in the input group correction file to RING. Symmetry correction values, which are corrections to the rotational entropy that arise from indistinguishable atoms in a molecule, were separately incorporated for calculating $dS_{alkoxide}$. Adsorption enthalpies and entropies obtained from RING showed good agreement with those reported by Nguyen et al.[33] using DFT calculations (Figure 1).

Table 2. Linear Dependencies of Carbon Number with Enthalpy (eq 2) and Entropy (eq 3) Difference between Alkoxide and Alkane Formation

enthalpy difference			entropy difference		
alkoxide	α	β	alkoxide	γ	η
1°	−4.4	26.80	all	−9.39	−157.43
2°	−4.4	9.13			
internal 2°	−8.92	25.68			
3°	−1.78	25.86			

The kinetics of olefin cracking on H-ZSM-5 were quantitatively assessed for β-scission modes C−F (Scheme 1b) by simultaneously solving four equations from butene, pentene (2-pentene and 2-methyl-2-butene feeds), and hexene (1-hexene, *trans*-4-methyl-2-pentene, and 2,3-dimethyl-2-butene) cracking (Table 1), assuming β-scission rate constants to be independent of carbon chain length, and β-scission modes to be lumped as a single mode, e.g., submodes E1 and E2 lumped as mode E. These experiments were conducted at differential conversion in the presence of olefin isomerization, however, with minimal olefin oligomerization and hydride transfer reactions as stoichiometric ratios of primary cracking products were observed in the effluent and only trace amounts of higher olefins were observed, if any at all.

3.1. Butene Cracking: Kinetics of Mode F. The rate constants for β-scission mode F were inferred from 1-butene cracking reactions on H-ZSM-5 (Table 3). Isomerization of the 1-butene feed was observed; among the isomers of butene, only 1-butene undergoes β-scission reactions via cracking mode F to form two molecules of ethene. Higher olefins were absent from the effluent stream, indicating that ethene was formed from elementary step β-scission reactions and not from secondary oligomerization and cracking reactions. Intrinsic activation barriers of cracking mode F were obtained from intrinsic rate constant values at various temperatures calculated using eq 7; an Arrhenius plot is shown in Figure 2a. The fractional surface coverage was low ($<10^{-6}$), and the partial pressure of 1-butene was determined from the effluent stream.

$$F_{oC_2^=} = k_F K_{1\text{-}C_4^=} P_{1\text{-}C_4^=} w_T \quad (7)$$

The intrinsic activation energy of β-scission mode F (E_{inF}) on H-ZSM-5 obtained in this study (257 ± 19 kJ mol^{-1}) showed good agreement with previously reported results from theoretical calculations: 238 kJ mol^{-1} reported by Lesthaeghe et al.[17] using ONIOM(B3LYP/6-31g(d):MNDO) methods and 236 kJ mol^{-1} reported by Vandichel et al.[45] using ONIOM(B3LYP/6-31+g(d):HF/6-31+g(d)) methods. The adsorption enthalpy of 1-butene (116 kJ mol^{-1})[33] has been added to both values that are reported as apparent activation energies.

3.2. Pentene Cracking: Kinetics of Mode D. A set of experiments analogous to those conducted for butene cracking was performed for pentene cracking over H-ZSM-5 (Table 1) to infer the rate constants of mode D cracking. The effluent streams when feeding 2-pentene and 2-methyl-2-butene over the zeolite (<1% conversion, at 773−803 K) contained a 1:1 ethylene:propene ratio and a nonequilibrium distribution of pentene isomers. Minimal C_{5+} hydrocarbons were detected in the effluent stream, indicating that the ethylene and propene observed in the effluent are formed in elementary step β-scission reactions of C_5 isomers. The various pentene isomers can crack through either mode F or mode D, and some isomers of pentene cannot undergo cracking; for example, 1-pentene can crack through mode F or D, depending on where the double bond is protonated (Scheme 1c). The identity and concentration of pentene isomers in the effluent stream were quantified by gas chromatography and mass spectrometry to account for the individual contribution of each pentene isomer in synthesizing ethene and propene. Cracking rate constants of mode D (k_D) were then determined from eq 8 with k_F values taken from 1-butene cracking.

dx.doi.org/10.1021/cs500119n | ACS Catal. 2014, 4, 2319−2327

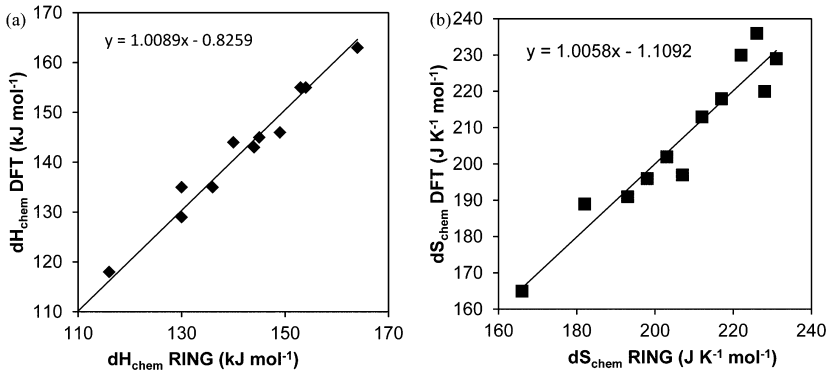

Figure 1. Parity plots of (a) chemisorption enthalpies and (b) entropies reported by Nguyen et al.[32,33] vs those calculated using RING.

Table 3. Comparison of Kinetic Parameters of β-Scission Modes C−F

	k_{in} (s^{-1})	E_{in} (kJ mol^{-1})	
cracking mode	experiment (783 K)	experiment	computational studies
F (1° to 1°)	1.9×10^2	257 ± 19	238[17]
			236[45]
D (1° to 2° and 2° to 1°)	1.5×10^3	193 ± 13	D_1, 196[11]
			D_2, 233[11]
			D_2, 183[46]
C (2° to 2°)	3.1×10^4	185 ± 4	161[11]
E (1° to 3° and 3° to 1°)	1.6×10^6	160 ± 7	E_1, 144[11]
			E_2, 200[11]

$$F_{oC_3^=} = (k_D K_{C/T\text{-}2\text{-}C_5^=} P_{C/T\text{-}2\text{-}C_5^=} + k_D K_{3\text{-}C_1\text{-}1\text{-}C_4^=} P_{3\text{-}C_1\text{-}1\text{-}C_4^=} + k_D K_{1\text{-}C_5^=} P_{1\text{-}C_5^=} + k_F K_{1\text{-}C_5^=} P_{1\text{-}C_5^=} + k_F K_{2\text{-}C_1\text{-}1\text{-}C_4^=} P_{2\text{-}C_1\text{-}1\text{-}C_4^=}) w_T \quad (8)$$

Intrinsic activation energies of mode D (E_{inD}) on H-ZSM-5 (193 ± 13 kJ mol^{-1}) derived from an Arrhenius plot using k_D values assessed using both 2-pentene and 2-methyl-2-butene as feeds (Figure 2b) are comparable to the values of 196 and 233 kJ mol^{-1} for modes D_1 and D_2, respectively, reported by Mazar et al.[11] using PBE-D DFT calculations and the value of 183 kJ mol^{-1} for 1-hexene cracking via mode D_2 reported by Guo et al.[46] using ONIOM(B3LYP/6-31G(d,p):UFF) methods and an 88T MFI cluster.

3.3. Hexene Cracking: Kinetics of Modes C and E. A set of experiments analogous to those conducted for butene and pentene cracking was performed for 1-hexene, *trans*-4-methyl-2-pentene, and 2,3-dimethyl-2-butene cracking over H-ZSM-5 (Table 1) to infer rate constants of cracking modes C and E. We observed a 1:1 ethene:butene molar ratio and a nonequilibrium distribution of hexene isomers in the effluent stream. The concentrations of hexene isomers in the effluent depend strongly on the hexene feed (Figure S2 of the Supporting Information): a more branched olefin isomer feed was less likely to isomerize into an olefin isomer with a different structural backbone, because of the size restrictions imposed by the microporous voids of the zeolite, and thereby result in a nonequilibrium olefin isomer distribution. The product selectivities of the various hexene feeds at 783 K, however, were consistent with each other (Table 4) and comparable to

Table 4. Selectivities for Ethene, Propene, and Butenes from Hexene Cracking at 783 K

hexene isomer feed	conversion (%)	$C_2^=$:$C_3^=$:$C_4^=$
1-hexene	10	9.6:80.9:9.5
trans-4-methyl-2-butene	15	9.0:82.0:9.0
2,3-dimethyl-2-butene	3	9.6:80.8:9.6

that reported by Buchanan et al.[13] for 1-hexene cracking on H-ZSM-5 at 783 K (7:83.6:7.9 ethene:propene:butene ratio at 20.1% conversion). A total of 10 of 17 possible hexene isomer peaks were identified in the effluent to close the carbon balance ±5%.

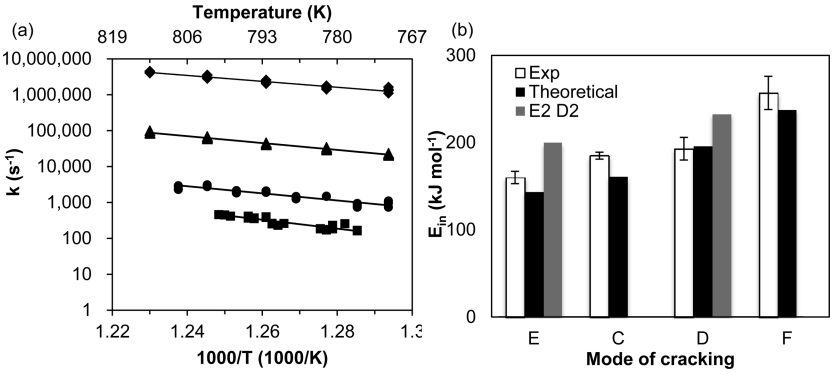

Figure 2. Intrinsic rate constant and activation energy of β-scission modes C−F from butene, pentene, and hexene cracking on H-ZSM-5 at 773−813 K. (a) Arrhenius plots of intrinsic rate constants (◆) k_E, (▲) k_C, (●) k_D, and (■) k_F. (b) Comparison of intrinsic activation energies with DFT calculations: (white) current finding, (black) computational values for E_1 and D_1, and (gray) computational values for E_2 and D_2.[11,17]

dx.doi.org/10.1021/cs500119n | ACS Catal. 2014, 4, 2319−2327

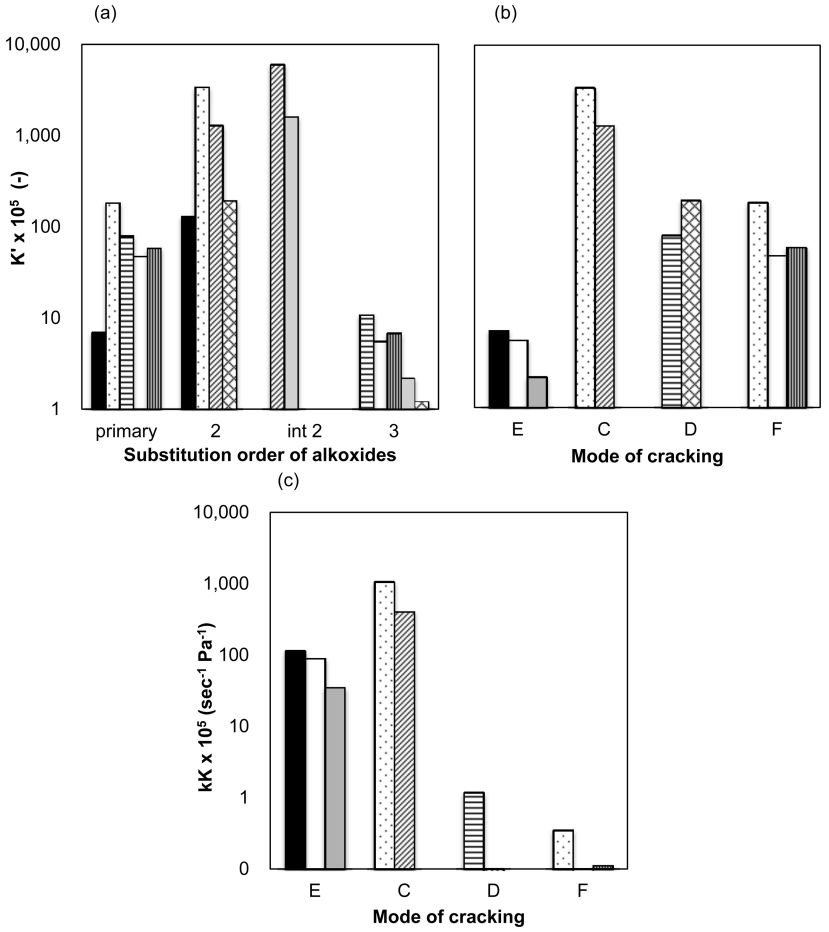

Figure 3. Adsorption constants of (a) primary, secondary, internal secondary, and tertiary hexoxides; (b) eight C_6 olefin isomers identified that can undergo β-scission. (c) Apparent rate constants of the eight olefins. [K (Pa^{-1}) = K' (−) × 10^{-5} (Pa^{-1})] (black) 3,3-diC_1-1-$C_{4=}$, (white) 2-C_1-1-$C_{5=}$, (gray) 2-C_1-2-$C_{5=}$, (dotted) 4-C_1-1-$C_{5=}$, (horizontal lines) 2,3-diC_1-1-$C_{4=}$, (vertical lines) 2-C_2-1-$C_{4=}$, (diagonal lines) *trans*-4-C_1-2-$C_{5=}$, (crosshatched) *trans*-3-C_1-2-$C_{5=}$. All adsorption constants reported herein were evaluated at 783 K.

Rate constants of cracking types C and E were obtained by taking the hexene partial pressures measured in the effluent stream and k_D and k_F values from pentene and butene cracking results to simultaneously solve eqs 9 and 10.

$$0.5F_{oC_3^=} = (k_C K_{T\text{-}4\text{-}C_1\text{-}2\text{-}C_5^=} P_{T\text{-}4\text{-}C_1\text{-}2\text{-}C_5^=} + k_C K_{4\text{-}C_1\text{-}1\text{-}C_5^=} P_{4\text{-}C_1\text{-}1\text{-}C_5^=} + k_D K_{2,3\text{-}diC_1\text{-}1\text{-}C_4^=} P_{2,3\text{-}diC_1\text{-}1\text{-}C_4^=} + k_F K_{2\text{-}C_1\text{-}1\text{-}C_5^=} P_{2\text{-}C_1\text{-}1\text{-}C_5^=}) w_T \quad (9)$$

$$F_{oC_2^=} = (k_E K_{3,3\text{-}diC_1\text{-}1\text{-}C_4^=} P_{3,3\text{-}diC_1\text{-}1\text{-}C_4^=} + k_E K_{2\text{-}C_1\text{-}1\text{-}C_5^=} P_{2\text{-}C_1\text{-}1\text{-}C_5^=} + k_E K_{2\text{-}C_1\text{-}2\text{-}C_5^=} P_{2\text{-}C_1\text{-}2\text{-}C_5^=} + k_D K_{T\text{-}3\text{-}C_1\text{-}2\text{-}C_5^=} P_{T\text{-}3\text{-}C_1\text{-}2\text{-}C_5^=} + k_F K_{4\text{-}C_1\text{-}1\text{-}C_5^=} P_{4\text{-}C_1\text{-}1\text{-}C_5^=} + k_F K_{2\text{-}C_2\text{-}1\text{-}C_4^=} P_{2\text{-}C_2\text{-}1\text{-}C_4^=}) w_T \quad (10)$$

Activation energies of mode C (E_{inC}) (185 ± 4 kJ mol^{-1}) and E (E_{inE}) (160 ± 7 kJ mol^{-1}) were obtained from temperature dependence plots of the rate constants using cracking data from the three hexene isomer feeds (Figure 2a). These numbers compare favorably with those calculated using PBE-D DFT by Mazar et al.,[11] who reported values of 144 and 200 kJ mol^{-1} for modes E_1 and E_2, respectively, and 161 kJ mol^{-1} for mode C (Figure 2b). Rate constants k_E and k_C obtained using three different hexene isomers as feeds plotted in Figure 2a are consistent, and this consistency in rate constants shows that even though the degree of isomerization varies when using different isomers as the primary feed, accounting for the adsorption and kinetics of each isomer in the effluent stream allows for the evaluation of intrinsic β-scission rate constants.

Comparing activation energies E_{inE1}, E_{inE2}, E_{inD1}, and E_{inD2} of Mazar et al.[11] (Figure 2b) shows that experimental values reported here agree better with modes E_{inE1} and E_{inD1} where the primary alkoxide is involved in the reactant state and the more substituted β C (tertiary and secondary) is involved in the transition state,[11] implying that modes E_1 and D_1 are more dominant in lumped groups E and D, respectively, because their activation barriers are lower than those of E_{inE2} and E_{inD2}.

3.4. Chemisorption and Apparent Rate Constants for Cracking of Hexene Isomers. An examination of the chemisorption equilibrium constants of all adsorption modes of the eight hexene isomers, among the 10 identified, that are viable for β-scission (Figure 3a) showed that, in general, the adsorption of secondary alkoxides is favored over that of primary and tertiary alkoxides, which are the least favorable. The ratio of the largest adsorption constants at 783 K among internal secondary, secondary, primary, and tertiary alkoxides is 555:314:17:1 from *trans*-4-methyl-2-pentene, 4-methyl-1-pentene, 4-methyl-1-pentene, and 2,3-dimethyl-1-butene, respectively. A closer examination of only the adsorption modes available to crack among the eight hexene isomers against the four modes of cracking reveals that olefins that undergo

dx.doi.org/10.1021/cs500119n | ACS Catal. 2014, 4, 2319−2327

Table 5. Averaged Fractional Contributions from Different Modes of Cracking to Hexene Cracking Products between 783 and 813 K

	cracking product $2C_3$			cracking products C_2 and C_4		
	cracking mode C	cracking mode D	cracking mode F	cracking mode E	cracking mode D	cracking mode F
2,3-dimethyl-2-butene	0.9874	0.0125	0.0001	0.9752	0.0238	0.0010
trans-4-methyl-2-butene	0.9992	0.0006	0.0002	0.9653	0.0332	0.0012
1-hexene	0.9992	0.0006	0.0002	0.9660	0.0327	0.0013

cracking via mode E have the fastest intrinsic rate constant but the lowest adsorption constant (Figure 3b).

A comparison of the apparent rate constants of hexene cracking, k_iK_j (s^{-1} Pa^{-1}) (i, mode E, C, D, or F; j, the corresponding hexene isomer) (Figure 3c) shows that (i) olefins that crack through mode C have apparent rate constants larger than those of mode E and (ii) the contributions from cracking modes D and F can be neglected under the reaction conditions considered (773−813 K). A comparison of cracking mode C that forms two propene molecules and mode E that forms ethene and butene from hexene cracking reveals that the largest apparent rate constants involve $k_CK_{4\text{-methyl-1-pentene}}$ and $k_EK_{3,3\text{-dimethyl-1-butene}}$ in a 9:1 ratio at 783 K, which is consistent with experimental observations in which the measured ratio of propene to ethene synthesis is 8:1 at 783 K. This implies that the observed product distribution of olefin cracking involves the interplay between olefin chemisorption constants and the intrinsic β-scission rate constant. Hence, the assumption that the most favorable mode of cracking, mode E, predominates over other modes is invalid for H-ZSM-5.

The conversion of 2,3-dimethyl-2-butene (<3%, 48 Pa), which does not have any available modes of cracking, was much lower than of 1-hexene (<10%, 38 Pa) and *trans*-4-methyl-2-pentene (<15%, 34 Pa) feeds, and the unreacted feed accounted for ∼50% of all the hexene isomers in the effluent. A further comparison of the fractional contributions to propene and ethene syntheses from the four modes of β scission in hexene cracking (Table 5) reveals that when using 2,3-dimethyl-2-butene as the primary feed, the fractional contributions are different from those using 1-hexene and *trans*-4-methyl-2-pentene. These differences coincide with the isomer distributions of each of the feeds (Figure S2 of the Supporting Information) measured in the effluent in hexene cracking. The 2,3-dimethyl-2-butene feed has extreme isomer distributions (∼50% of 2,3-dimethyl-2-butene and ∼23% of 2,3-dimethyl-1-butene) compared to those observed when using 1-hexene and *trans*-4-methyl-2-pentene (both feeds have ∼6% of 2,3-dimethyl-2-butene and ∼3% of 2,3-dimethyl-1-butene in the effluent stream) as primary feeds, which demonstrates that (i) different carbon backbones of hexene feeds may result in different extents of olefin isomerization and (ii) besides apparent rate constants of olefin cracking, the concentrations of the dominant precursors can also significantly influence cracking rates.

4. CONCLUSIONS

Linear relationships between alkoxide and alkane enthalpy and entropy of formation were proposed to estimate olefin adsorption constants on H-ZSM-5 based on group additivity and group correction methods, which, in general, can be applied to surface chemistries on zeolitic solid acids with specific numbers reported here applicable to H-ZSM-5. Intrinsic β-scission rate constants of modes C−F were inferred from cracking of linear and branched isomers of butene, pentene, and hexene at low conversions (<15%) over a temperature range of 773−813 K by simultaneously solving for the observed concentration of cracking products analytically and concurrently accounting for the nonequilibrium distribution of olefin isomers in the effluent stream with the assumption that intrinsic rate constants are independent of carbon chain length. Intrinsic activation energies calculated from Arrhenius plots showed good agreement with computational calculations. The intrinsic rate parameters of β-scission modes were dominated by the substitution order of the reactant and product alkoxides, wherein $E_{inE} < E_{inC} < E_{inD} < E_{inF}$ and the k_E:k_C:k_D:k_F ratio is 1094:21:8:1 at 783 K. Secondary alkoxides were found to have adsorption constants higher than those of primary and tertiary alkoxides, which is the least favorable adsorption mode. The apparent rate constants, k_iK_j (s^{-1} Pa^{-1}), of mode C were found to be ∼9 times larger than that of mode E; however, the intrinsic rate constant of mode E is ∼52 times larger than that of mode C (k_E:k_C ratio of 52:1 at 783 K). The varying extents of olefin isomerization observed in olefin cracking using different hexene feeds affect the fractional contribution of the four modes of β-scission to the cracking products, which demonstrates that the concentration of dominant olefin cracking precursors is also an important factor in determining olefin cracking rates.

■ ASSOCIATED CONTENT

Supporting Information

N_2 adsorption measurements with BET fit parameters, dimethyl ether titration of acid sites of the zeolite, XRD pattern of the zeolite, hexene isomer distributions, assessment of internal and external mass transfer limitations, discussion of relaxing the assumption of intrinsic rate constants being independent of carbon chain length, and parameters used for finding linear relationships for adsorption enthalpy and entropy. This material is available free of charge via the Internet at http://pubs.acs.org.

■ AUTHOR INFORMATION

Corresponding Author

*E-mail: abhan@umn.edu.

Notes

The authors declare no competing financial interest.

■ ACKNOWLEDGMENTS

We acknowledge financial support from The Dow Chemical Co. and the National Science Foundation (NSF CBET 1055846). We also acknowledge Dr. Mark N. Mazar for helpful technical discussions.

■ REFERENCES

(1) Koempel, H.; Liebner, W. Lurgi's Methanol To Propylene (MTP®) Report on a successful commercialisation. In *Studies of Surface Science and Catalysis*; Fábio Bellot Noronha, M. S., Eduardo

Falabella, S.-A., Eds.; Elsevier: Amsterdam, 2007; Vol. *167*, pp 261−267.
(2) Keil, F. J. *Microporous Mesoporous Mater.* **1999**, *29*, 49−66.
(3) Quann, R. J.; Green, L. A.; Tabak, S. A.; Krambeck, F. J. *Ind. Eng. Chem. Res.* **1988**, *27*, 565−570.
(4) Pines, H. *The chemistry of catalytic hydrocarbon conversions*; Academic Press: New York, 1981.
(5) Bessell, S.; Seddon, D. *J. Catal.* **1987**, *105*, 270−275.
(6) Guisnet, M.; Andy, P.; Gnep, N. S.; Benazzi, E.; Traver, C. *Oil Gas Sci. Technol.* **1999**, *54*, 23−28.
(7) Corma, A.; Orchillés, A. V. *Microporous Mesoporous Mater.* **2000**, *35*−*36*, 21−30.
(8) Greensfelder, B. S.; Voge, H. H. *Ind. Eng. Chem.* **1945**, *37*, 1038−1043.
(9) Thomas, C. L. *Ind. Eng. Chem.* **1949**, *41*, 2564−2573.
(10) Buchanan, J. S. *Appl. Catal.* **1991**, *74*, 83−94.
(11) Mazar, M. N.; Al-Hashimi, S.; Cococcioni, M.; Bhan, A. *J. Phys. Chem. C* **2013**, *117*, 23609−23620.
(12) Weitkamp, J.; Jacobs, P. A.; Martens, J. A. *Appl. Catal.* **1983**, *8*, 123−141.
(13) Buchanan, J. S.; Santiesteban, J. G.; Haag, W. O. *J. Catal.* **1996**, *158*, 279−287.
(14) Frash, M. V.; Kazansky, V. B.; Rigby, A. M.; van Santen, R. A. *J. Phys. Chem. B* **1998**, *102*, 2232−2238.
(15) Rigby, A. M.; Kramer, G. J.; van Santen, R. A. *J. Catal.* **1997**, *170*, 1−10.
(16) Frash, M. V.; van Santen, R. A. *Top. Catal.* **1999**, *9*, 191−205.
(17) Lesthaeghe, D.; Van der Mynsbrugge, J.; Vandichel, M.; Waroquier, M.; Van Speybroeck, V. *ChemCatChem* **2011**, *3*, 208−212.
(18) Natal-Santiago, M. A.; Alcalá, R.; Dumesic, J. A. *J. Catal.* **1999**, *181*, 124−144.
(19) Simonetti, D. A.; Ahn, J. H.; Iglesia, E. *J. Catal.* **2011**, *277*, 173−195.
(20) Kissin, Y. V. *Catal. Rev.: Sci. Eng.* **2001**, *43*, 85−146.
(21) Garwood, W. E. In *Conversion of C2-C10 to Higher Olefins over Synthetic Zeolite ZSM-5*; American Chemical Society: Washington, DC, 1983; pp 383−396.
(22) Berend, S.; Theo, L. M. M. *Nature* **2008**, *451*, 671−678.
(23) Benson, S. W. *Thermochemical kinetics; methods for the estimation of thermochemical data and rate parameters*; Wiley: New York, 1968.
(24) Marsi, I.; Viskolcz, B.; Seres, L. *J. Phys. Chem. A* **2000**, *104*, 4497−4504.
(25) Cohen, N.; Benson, S. W. *Chem. Rev.* **1993**, *93*, 2419−2438.
(26) Benson, S. W. *Chem. Rev.* **1978**, *78*, 23−35.
(27) Kua, J.; Faglioni, F.; Goddard, W. A. *J. Am. Chem. Soc.* **2000**, *122*, 2309−2321.
(28) Salciccioli, M.; Chen, Y.; Vlachos, D. G. *J. Phys. Chem. C* **2010**, *114*, 20155−20166.
(29) Salciccioli, M.; Edie, S. M.; Vlachos, D. G. *J. Phys. Chem. C* **2012**, *116*, 1873−1886.
(30) Fernández, E. M.; Moses, P. G.; Toftelund, A.; Hansen, H. A.; Martínez, J. I.; Abild-Pedersen, F.; Kleis, J.; Hinnemann, B.; Rossmeisl, J.; Bligaard, T.; Nørskov, J. K. *Angew. Chem., Int. Ed.* **2008**, *47*, 4683−4686.
(31) Abild-Pedersen, F.; Greeley, J.; Studt, F.; Rossmeisl, J.; Munter, T. R.; Moses, P. G.; Skúlason, E.; Bligaard, T.; Nørskov, J. K. *Phys. Rev. Lett.* **2007**, *99*, 016105.
(32) Nguyen, C. M.; De Moor, B. A.; Reyniers, M. F.; Marin, G. B. In *Effect of nanopore dimension and network topology on alkene sorption thermodynamics*; 2nd International Workshop (NAPEN-2011), Rodos, Greece; Ghent University: Ghent, Belgium, 2011; pp 28−32.
(33) Nguyen, C. M.; De Moor, B. A.; Reyniers, M. F.; Marin, G. B. *J. Phys. Chem. C* **2011**, *115*, 23831−23847.
(34) Nguyen, C. M.; De Moor, B. A.; Reyniers, M. F.; Marin, G. B. *J. Phys. Chem. C* **2012**, *116*, 18236−18249.
(35) De Moor, B. A.; Reyniers, M. F.; Gobin, O. C.; Lercher, J. A.; Marin, G. B. *J. Phys. Chem. C* **2011**, *115*, 1204−1219.
(36) De Moor, B. A.; Reyniers, M. F.; Marin, G. B. *Phys. Chem. Chem. Phys.* **2009**, *11*, 2939−2958.
(37) Rangarajan, S.; Bhan, A.; Daoutidis, P. *Comput. Chem. Eng.* **2012**, *45*, 114−123.
(38) Rangarajan, S.; Bhan, A.; Daoutidis, P. *Comput. Chem. Eng.* **2012**, *46*, 141−152.
(39) Rangarajan, S.; Bhan, A.; Daoutidis, P. *Ind. Eng. Chem. Res.* **2010**, *49*, 10459−10470.
(40) Sabbe, M. K.; De Vleeschouwer, F.; Reyniers, M.-F. o.; Waroquier, M.; Marin, G. B. *J. Phys. Chem. A* **2008**, *112*, 12235−12251.
(41) Sabbe, M. K.; Saeys, M.; Reyniers, M.-F.; Marin, G. B.; Van Speybroeck, V.; Waroquier, M. *J. Phys. Chem. A* **2005**, *109*, 7466−7480.
(42) Khan, S. S.; Yu, X.; Wade, J. R.; Malmgren, R. D.; Broadbelt, L. J. *J. Phys. Chem. A* **2009**, *113*, 5176−5194.
(43) Chiang, H.; Bhan, A. *J. Catal.* **2010**, *271*, 251−261.
(44) Berger, R. J.; Pérez-Ramírez, J.; Kapteijn, F.; Moulijn, J. A. *Chem. Eng. Sci.* **2002**, *57*, 4921−4932.
(45) Vandichel, M.; Lesthaeghe, D.; Van der Mynsbrugge, J.; Waroquier, M.; Van Speybroeck, V. *J. Catal.* **2010**, *271*, 67−78.
(46) Guo, Y. H.; Pu, M.; Chen, B. H.; Cao, F. *Appl. Catal., A* **2013**, *455*, 65−70.